Identification by NMR of the Binding Surface for the Histidine-Containing Phosphocarrier Protein HPr on the N-Terminal Domain of Enzyme I of the *Escherichia coli* Phosphotransferase System†

Daniel S. Garrett,‡ Yeong-Jae Seok,§ Alan Peterkofsky,§ G. Marius Clore,*,‡ and Angela M. Gronenborn*,‡

Laboratory of Chemical Physics, Building 5, National Institute of Diabetes and Digestive and Kidney Diseases, and Laboratory of Biochemical Genetics, Building 36, National Heart, Lung, and Blood Institute, National Institutes of Health, Bethesda, Maryland 20892

Received January 30, 1997⊗

ABSTRACT: The interaction between the ∼30 kDa N-terminal domain of enzyme I (EIN) and the ∼9.5 kDa histidine-containing phosphocarrier protein HPr of the *Escherichia coli* phosphoenolpyruvate:sugar phosphotransferase system has been investigated by heteronuclear magnetic resonance spectroscopy. The complex is in fast exchange, permitting us to follow the chemical shift changes of the backbone NH and ^{15}N resonances of EIN upon complex formation by recording a series of ^{1}H−^{15}N correlation spectra of uniformly ^{15}N-labeled EIN in the presence of increasing amounts of HPr at natural isotopic abundance. The equilibrium association constant derived from analysis of the titration data is $\sim 1.5 \times 10^5$ M^{-1}, and the lower limit for the dissociation rate constant is 1100 s^{-1}. By mapping the backbone chemical shift perturbations on the three-dimensional solution structure of EIN [Garrett, D. S., Seok, Y.-J., Liao, D.-I., Peterkofsky, A., Gronenborn, A. M., & Clore, G. M. (1997) *Biochemistry 36*, 2517−2530], we have identified the binding surface of EIN in contact with HPr. This surface is primarily located in the α domain and involves helices H1, H2, and H4, as well as the hinge region connecting helices H2 and H2′. The data also indicate that the active site His 15 of HPr must approach the active site His 189 of EIN along the shallow depression at the interface of the α and α/*β* domains. Interestingly, both the backbone and side chain resonances (assigned from a long-range ^{1}H−^{15}N correlation spectrum) of His 189, which is located at the N-terminus of helix H6 in he α/*β* domain, are only minimally perturbed upon complexation, indicating that His 189 (in the absence of phosphorylation) does not undergo any significant conformational change or change in pK_a value upon HPr binding. On the basis of results of this study, as well as a previous study which delineated the interaction surface for EI on HPr [van Nuland, N. A. J., Boelens, R., Scheek, R. M., & Robillard, G. T. (1995) *J. Mol. Biol. 246*, 180−193], a model for the EIN/HPr complex is proposed in which helix 1 (residues 16−27) and the helical loop (residues 49−53) of HPr slip between the two pairs of helices constituting the α domain of EIN. In addition, we suggest a functional role for the kink between helices H2 and H2′ of EIN, providing a flexible joint for this interaction to take place.

The transport of numerous sugars across the cytoplasmic membrane of bacterial cells is coupled to phosphoryl transfer from phosphoenolpyruvate (PEP)[1] via several protein intermediates to these sugar molecules [see Postma et al. (1993) and Herzberg and Klevit (1994) for reviews]. Enzyme I (EI), the first protein in the phosphorylation cascade, is autophosphorylated by PEP at His 189 (*Escherichia coli* numbering scheme). Phospho-EI acts as the phosphoryl donor to His 15 (*E. coli* numbering scheme) of the histidine-containing phosphocarrier protein HPr. Phospho-HPr in turn donates the phosphoryl group to the sugar transporters, collectively known as enzymes II (EIIs). Over the last few years, considerable effort has been devoted to elucidating structural details of the various protein components of the PTS system, and three-dimensional structures for both HPr (Klevit & Waygood, 1986; Hammen et al., 1991; Wittekind et al., 1992; Herzberg et al., 1992; Jia et al., 1993; van Nuland et al., 1994, 1995) and EIIs (Liao et al., 1991; Worthylake et al, 1991; Fairbrother et al., 1992) from various sources have been determined by NMR and X-ray crystallography. More recently, crystal (Liao et al., 1996) and solution NMR (Garrett et al., 1997) structures of the ∼30 kDa amino-terminal domain of enzyme I (EIN) of *E. coli* have been determined. EIN can reversibly phosphorylate HPr although it has lost its ability to become phosphorylated by PEP (Seok et al., 1996; Chauvin et al., 1996). In addition, EIN is capable of functioning in phosphotransfer reactions with a variety of acceptor proteins which cannot be phosphorylated by intact EI (Seok et al., 1996). Thus, it appears that the general ability to interact with protein substrates and transfer the phosphoryl group resides in the N-terminal domain of EI, whereas the binding site for PEP and modulation of the general activity of EI are associated with the C-terminal domain. In order to shed light on the mechanism of

† This work was supported in part by the AIDS Targeted Anti-Viral Program of the Office of the Director of the National Institutes of Health (G.M.C. and A.M.G.).

* Authors to whom correspondence should be addressed (e-mail: G.M.C., clore@vger.niddk.nih.gov; A.M.G., gronenborn@vger.niddk.nih.gov).

‡ Laboratory of Chemical Physics.

§ Laboratory of Biochemical Genetics.

⊗ Abstract published in *Advance ACS Abstracts,* April 1, 1997.

[1] Abbreviations: PTS, phosphoenolpyruvate:sugar phosphotransferase system of *Escherichia coli*; EI, enzyme I of the PTS; EIN, N-terminal domain (residues 1−259) of EI; EII(s), enzyme(s) II of the PTS; HPr, histidine-containing phosphocarrier protein of the PTS; PEP, phosphoenolpyruvate; NMR, nuclear magnetic resonance; HSQC, heteronuclear single-quantum coherence; U-^{15}N protein, uniformly ^{15}N-labeled (>95%) protein; U-^{14}N protein, protein with the nitrogen atoms at natural isotopic abundance.

S0006-2960(97)00221-3

phosphotransfer between two protein components, it is important to characterize the regions of the two proteins which constitute the binding interface during phosphoryl transfer. In this paper, we investigate the interaction between EIN and HPr by NMR, determine the association constant between the two proteins, identify the binding surface of HPr on EIN, and propose a model for the interaction.

EXPERIMENTAL PROCEDURES

Construction of the HPr Expression Vector pSP100. The coding sequence for *E. coli* HPr (nt 205−486 of the *pts*H gene) was amplified by PCR using pDS20 (Reddy et al., 1991) as a template. The forward PCR primer 5′-GGAAATCATATGTTCCAGCAAGAAGTTACCATT-ACCGCTCCGAACGT-3′ contained an engineered *Nde*I restriction site (underlined), and the reverse primer 5′-AAAGAACCCGGG**TTA***TTA*CTCGAGTTC-3′ contained an engineered stop codon (in bold) in addition to a preexisting stop codon (in italics) and *Sma*I and *Xho*I restriction sites (underlined). The *Nde*I- and *Sma*I-cut PCR product was gel purified and ligated into the corresponding sites of the vector pRE2 (Reddy et al., 1991). *E. coli* strain GI698 was transformed with the recombinant plasmid as previously described (Seok et al., 1996).

Expression and Purification of HPr. Strain GI698/pSP100 was grown in defined medium, and HPr expression was induced with tryptophan (Seok et al., 1996). Cells were harvested by centrifugation, resuspended in 10 mM Tris, pH 7.5, and ruptured by two passages through a French pressure cell at 10 000 psi. After centrifugation, the supernatant was chromatographed on a MonoQ HR 10/10 column (Pharmacia) using 10 column volumes of 10 mM Tris, pH 7.5, with a linear salt gradient to 0.3 M NaCl. HPr-containing fractions were pooled, concentrated, and further purified on a Superose 12 gel filtration column in 10 mM Tris, pH 7.5, and 100 mM NaCl. The final product was >95% pure, as judged by SDS/PAGE electrophoresis.

Expression and Purification of EIN. EIN was expressed from the plasmid pLP2 in *E. coli* strain GI698 and purified as described previously (Seok et al., 1996). Uniformly (>95%) ^{15}N-labeled EIN was prepared as described in Garrett et al. (1997).

NMR Spectroscopy. All NMR experiments were carried out at 40 °C on a Bruker DMX600 spectrometer equipped with a triple gradient triple resonance probe. 2D ^{1}H−^{15}N HSQC spectra were recorded using a water flip-back as described by Grzesiek and Bax (1993). A 2D long-range ^{1}H−^{15}N HSQC spectrum to correlate the Nδ1 and Nϵ1 ring nitrogens with the Cϵ1H and Cδ2H ring protons of histidine was recorded with a 22 ms dephasing delay during which time the ^{1}H and ^{15}N signals become antiphase (Pelton et al., 1993). Spectra were processed with the NmrPipe package (Delaglio et al., 1995) and analysed using the programs PIPP, CAPP, and STAPP (Garrett et al., 1991).

RESULTS AND DISCUSSION

The pattern of resonance frequencies of individual nuclei for a particular protein can be regarded as a fingerprint of its structure. Indeed, the perturbation of ^{15}N and NH chemical shifts of uniformly ^{15}N-labeled proteins upon complex formation with another protein or ligand provides a highly sensitive tool for the mapping of binding sites (Chen et al., 1993; van Nuland et al., 1993, 1995; Gronenborn & Clore, 1993; Rajagopal & Klevit, 1994, Emerson et al., 1995; Grzesiek et al., 1996; Shuker et al., 1996).

Figure 1 shows the ^{1}H−^{15}N HSQC spectrum of the U-^{15}N EIN domain (blue contours) overlaid on that of the U-^{15}N EIN/U-^{14}N HPr complex (red contours). The complex is in fast exchange on the chemical shift scale, and the assignments of the ^{15}N and NH resonances in the complex were obtained by following the previously assigned cross peaks in the ^{1}H−^{15}N HSQC spectrum of uncomplexed EIN (Garrett et al., 1997) upon titration with increasing amounts of HPr up to a molar ratio of HPr to EIN of 1.62:1. The data in Figure 1 reveals two major classes of resonances: those that are shifted upon complexation and those which remain at essentially the same chemical shift positions as in free EIN. Since all the spectra were recorded under nearly identical buffer and temperature conditions, the observed shifts in the EIN resonances must arise either directly or indirectly from contacts with HPr.

A plot of the weighted average chemical shift change of the ^{1}H and ^{15}N resonances for selected cross peaks (the side chain amide of Gln 111 and backbone amides of Glu 83, Val 107, Ser 166, and His 189), given by $\Delta_{av} = [(\Delta\delta^2_{HN} + \Delta\delta^2_{N}/25)/2]^{1/2}$, as a function of the molar ratio of HPr to EIN is shown in Figure 2. The side chain amide of Gln 111 displays the largest weighted average shift perturbation upon complexation, while that for the backbone amide of the active site His 189 is approximately 40-fold less. A nonlinear least-squares best fit of these data to a simple one-site binding model given by EIN + HPr $\rightleftharpoons$ EIN/HPr yields an equilibrium association constant of $\sim 1.5 \times 10^5$ M^{-1}, in complete agreement with the results obtained by isothermal titration calorimetry (Chauvin et al., 1996). The maximum observed shift change is ~180 Hz (for the Hϵ21 proton of the side chain amide of Gln 111), yielding a lower limit of ~ 1100 s^{-1} for the dissociation rate constant (and a concomitant upper limit of $\sim 1.5 \times 10^8$ M^{-1} s^{-1} for the association rate constant). (Note that as the system is in fast exchange, $k_{diss} \gg 2\pi\Delta\delta$, where $\Delta\delta$ is the maximum observed difference in shift between the free and complexed forms of EIN.)

The ^{15}N and NH chemical shift changes observed upon complexation of U-^{15}N EIN with U-^{14}N HPr are color coded in Figure 3 on backbone tubular and molecular surface representations of EIN, clearly delineating the primary binding region for HPr on EIN. Residues with the largest chemical shift perturbations are indicated in yellow, and those that are unperturbed upon binding are shown in blue. EIN comprises two domains: an α domain (residues 33−143) consisting of a four-helix bundle made up of helices H1, H2/H2′, H3, and H4, and an α/β domain (residues 1−20 and 148−230) consisting of six β-strands and three α-helices (H5 to H7). The two domains are connected by linkers (residues 21−32 and 144−147). In addition, there is a C-terminal helix (H8, residues 233−250). EIN is elongated in shape, and the two domains are oriented at an angle of about 130° relative to each other, giving EIN an L-shaped appearance. The active site histidine at position 189 is located at the N-terminal end of helix H6 (residues 188−198) in the α/β domain. The interface between the α and α/β domains comprises helices H1, H2, and H4 of the α domain and helices H5 and H6, as well as some loops, of the α/β domain. The largest shift perturbations are observed

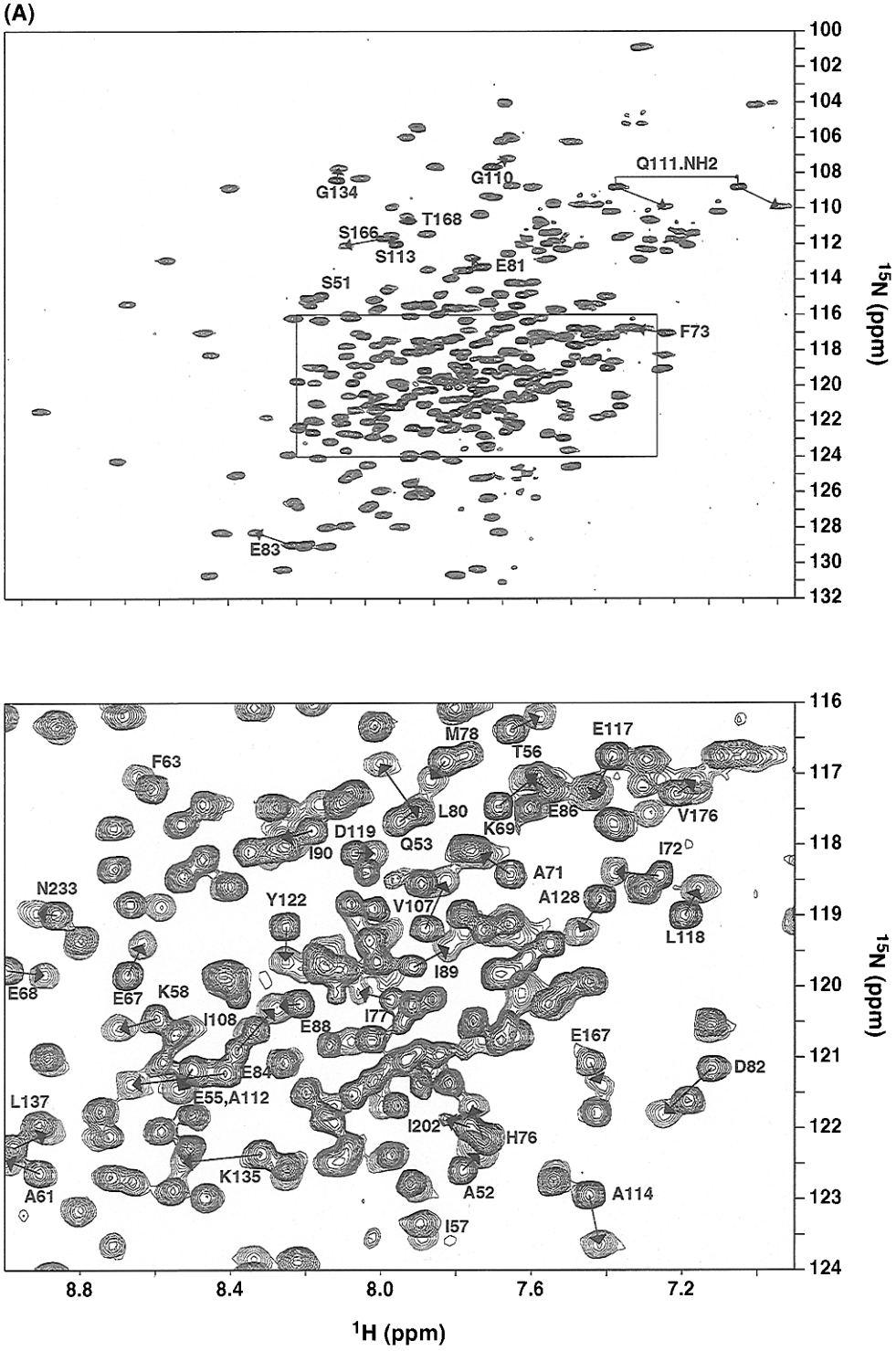

FIGURE 1: Superposition of the $^{1}H-^{15}N$ HSQC spectra of uncomplexed U-^{15}N EIN (blue) and the U-^{15}N EIN/U-^{14}N HPr complex (red) at a ratio of 1:1.6 EIn to HPr. Panel B corresponds to an expanded view of the boxed region in panel A. Cross peaks are labeled at their positions in free EIN, and the arrows connect the cross peaks of free EIN (blue) with the corresponding ones (red) in the complex. Both samples contained approximately 1 mM EIN in 20 mM sodium phosphate, pH 7.1, in 90% H_2O/10% D_2O, and the spectra were recorded at 40 °C.

in the α domain of EIN, in particular, in helices H2 (Lys 69, Ile 72, Phe 73, Leu 80, Glu81), H3 (Val 107, Ile 108, Gly 110, Gln 111, Ser 113, Ala 114, Glu 116, Glu 117), and H4 (Ala 128, Gly 134, Lys 135), and in the hinge between helices H2 and H2′ (Asp 82, Glu 83, Glu 84). The only significant shift changes in the α/β domain occur at the N-terminus of helix H5, involving Ser 166 which is in direct contact with Phe 73 of helix H2. These data therefore suggest that the primary binding site for HPr is located in the α domain and that HPr may approach the active site histidine (His 189) by slightly opening the cleft between the two pairs of helices constituting the four-helix bundle.

To determine whether the active site His 189 itself undergoes either a conformational change or a change in pK_a value upon HPr binding, long-range $^{1}H-^{15}N$ correlation spectra of U-^{15}N EIN and the U-^{15}N EIN/U-^{14}N HPr complex were recorded at pH 7.1 to correlate the ^{15}N shifts of the histidine side chain nitrogens with the Hϵ1 and Hδ2 ^{1}H shifts

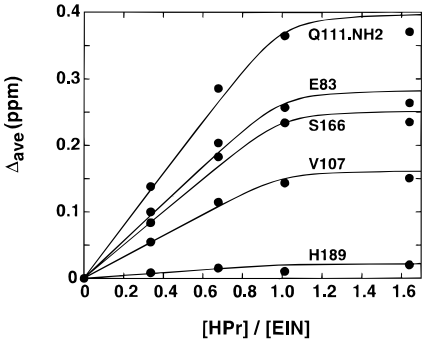

FIGURE 2: Weighted average of ^{1}H and ^{15}N chemical shifts of selected amide groups as well as the side chain amide group of Gln 111 as a function of the molar ratio of HPr to EIN. The weighted average of the ^{1}H and ^{15}N chemical shifts of a given residue is given by $\Delta_{av} = [(\Delta\delta^2_{NH} + \Delta\delta^2_N/25)/2]^{1/2}$ (Grzesiek et al., 1996).

of the carbon-attached protons of the imidazole ring (Figure 4). Only very minor chemical shift changes for the side chain of His 189, as well as the other histidine residues, are observed. The small chemical shift changes observed for the side chain of His 97 are most likely due to a very small difference in conformation and/or pK_a between free EIN and the EIN/HPr complex.

In both the NMR and X-ray structures of EIN, only the Nδ1 atom of the imidazole ring is accessible to solvent, and in addition, the Nϵ2 atom accepts a hydrogen bond from the hydroxyl proton of Thr 168 (Garrett et al., 1997; Liao et al., 1996). The data in Figure 4 indicate that the tautomeric state and conformation of His 189 remain unchanged upon complexation with HPr. Since EIN is phosphorylated at the Nϵ2 position of His 189 (Weigel et al., 1982a), the conformation of His 189 must change upon phosphorylation. There are two possibilities for such a conformational change. In the first, the χ_1 angle of His 189 remains unchanged in the trans rotamer, and a change in the χ_2 angle occurs; in the second, the χ_1 angle of His 189 changes from the trans to the g$^-$ rotamer. In the former case, the side chain of His 189 is located in the shallow depression (indicated by the arrow on the left-hand side of Figure 3D), while in the latter case it is located in the deep depression (indicated by the arrow on the right-hand side of Figure 3D) at the interface of the α and α/β domains. The shallow depression is located primarily between the two pairs of helices H1 and H2, and H4 and H3, whereas the deep depression is found between the back side of helices H3 and H4 and the linker connecting the α/β domain to the α domain. Liao et al. (1996) suggested in their modeling study of the EIN/HPr complex that HPr approaches from the shallow depression, since this required the fewest changes in backbone conformation. The present NMR data confirm this hypothesis as the major chemical shift perturbations occur in the vicinity of the shallow depression (Figure 3D).

Making use of the coordinates of the solution structure of EIN (Garrett et al., 1997; PDB accession code 1EZA) and the X-ray structure of *E. coli* HPr (Jia et al., 1993; PDB accession code 1POH), we modeled the complex of EIN and HPr. HPr was docked onto the EIN structure such that the two active site histidines were close enough to permit phosphoryl transfer and the contact regions on HPr (van Nuland et al., 1995) and EIN (present work) were in close proximity (Figure 5). It should be stressed that the model

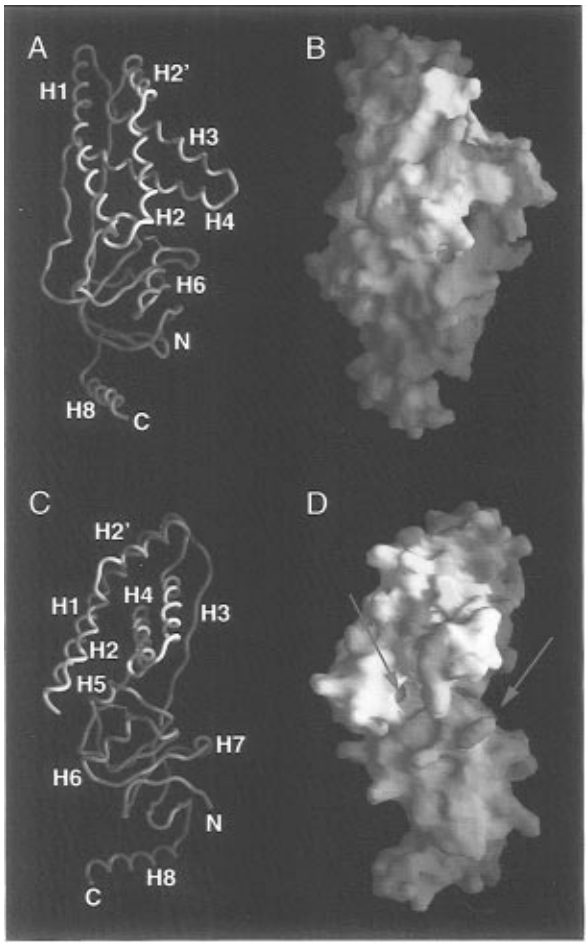

FIGURE 3: (A and C) Backbone tubular and (B and D) molecular surface representations of the solution structure of EIN delineating the binding surface for HPr. The color coding reflects the normalized weighted average of the ^{1}H and ^{15}N chemical shifts calculated as $[(\Delta\delta^2_{NH} + \Delta\delta^2_N/25)/2]^{1/2}/\Delta_{max}$, where Δ_{max} is the maximum observed weighted shift difference (0.37 ppm for the Nϵ2−Hϵ21 cross peak of Gln111). The colors range from yellow ($\Delta_{av}/\Delta_{max} = 1.0$) through gray ($\Delta_{av}/\Delta_{max} = 0.5$) to blue ($\Delta_{av}/\Delta_{max} = 0$). (A) and (B) show the same view; the view presented in (C) and (D) is rotated from that in (A) and (B) by ~90° around the long axis of the molecule. The side chain of the active site histidine at position 189 is shown in red in (A) and (C). The red arrows in (D) indicate the shallow (left) and deep (right) depressions that provide access to the active site histidine. This figure was generated with the program GRASP (Nicholls et al., 1991), and the coordinates of EIN employed are those of the solution NMR structure (PDB accession code 1EZA).

presented here is only intended as a cartoon depiction of the complex. The residues of HPr that experience the largest shifts upon complex formation with EI are located in two major areas (van Nuland et al., 1995). The first region involves the helix (residues 16−27) which follows the phosphoryl accepting His 15. The largest shifts in this region are observed for the backbone amides of His 15, Thr 16, Arg 17, Gln 21, and Lys 24. The second region comprises the helical loop (or one helical turn) around Leu 50, with Thr 52 exhibiting the largest shift. In addition, the backbone amide of Ala 82, located close to the C-terminus of HPr, experiences a significant perturbation upon EI binding (van Nuland et al., 1995). We docked the two areas of HPr onto the EIN structure, taking into account those residues in EIN which we identified as being in the contact region. The result is shown in Figure 5 in which helix 1 and the helical loop of HPr are positioned between the two pairs of helices of

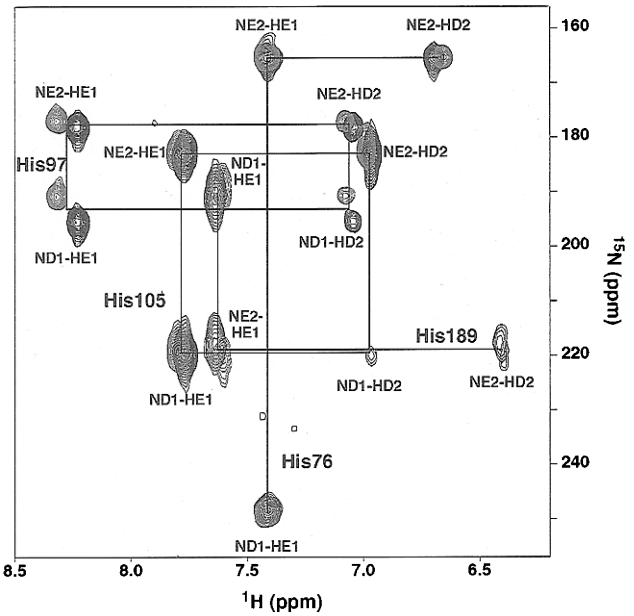

FIGURE 4: Superposition of the long-range $^{1}H-^{15}N$ correlation spectra of U-^{15}N EIN (blue) and the U-^{15}N EIN/U-^{14}N HPr complex (red) recorded at pH 7.1 and 40 °C. From the chemical shifts of the Nδ1 and Nϵ2 atoms, one can conclude that, in the unphosphorylated state of both free EIN and the EIN/HPr complex, the neutral species of His 189 is the Nδ1−H tautomer, while for His 76, His 97, and His 105 the neutral species is the Nϵ2−H tautomer.

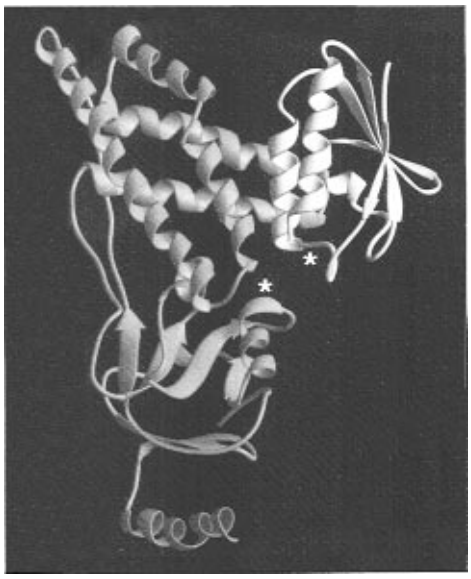

FIGURE 5: Ribbon diagram of a model of the EIN/HPr complex. EIN is shown in red, while HPr is shown in green. The locations of the two histidine residues involved in phosphoryl transfer, His 189 of EIN and His 15 of HPr, are indicated by stars. The two molecules were docked on the basis of the backbone amide chemical shift perturbations, as discussed in the text, using the programs FRODO (Jones, 1978) and GRASP (Nicholls et al., 1991). The figure was generated with the program RIBBONS (Carson, 1987). The model is only intended as a crude cartoon diagram. The Cα−Cα distance between His 189 and His 15 is ~11 Å in the model. In the unphosphorylated forms of EIN and HPr, His 189 and His 15 have χ_1/χ_2 angles of ~180°/60° and 45°/103°, respectively. His 189 and His 15 are phosphorylated at the Nϵ2 (Weigel et al., 1982a) and Nδ1 (Weigel et al., 1992b) positions, respectively. While the Nδ1 atom of His 15 is solvent accessible in free HPr, the Nϵ2 atom of His 189 is buried and accepts a hydrogen bond from the hydroxyl group of Thr 168 in the unphosphorylated forms of both free EIN and the EIN/HPr complex. Hence, the side chain conformation of His 189 must undergo a conformational change upon phosphorylation. In the current model of the EIN/HPr complex shown in this figure, changing the χ_1/χ_2 angles of His 189 and His 15 to −140°/−105° and 70°/105°, respectively, reduces the distance between the Nϵ2 atom of His 189 and the Nδ1 atom of His 15 to <5 Å, which is sufficiently close for phosphoryl transfer to occur. The coordinates employed are those of the solution NMR structure of EIN (Garrett et al., 1997; PDB accession code 1EZA) and the X-ray structure of *E. coli* HPr (Jia et al., 1993; PDB accession code 1POH).

the α domain of EIN. As can be appreciated, the proposed interaction also results in close proximity of the C-terminus of HPr with the N-terminal end of helix H2 of EIN, in complete agreement with the available mutational data which imply a role for the C-terminus in phosphoryl transfer (Anderson et al., 1991). The two histidine residues involved in phosphoryl transfer are indicated by the stars and are located potentially close enough to allow phosphoryl transfer to occur.

The orientation of HPr on EIN in our model differs from that proposed by Liao et al. (1996) in several respects. In the model of Liao et al. (1996), the sheets and helices of HPr are almost orthogonal to the long axis of EIN. In our model, on the other hand, helices H4 and H3 of EIN and the interacting helix of HPr (residues 16−27) are approximately orthogonal. In the Liao et al. (1996) model, the only contacts between HPr and EIN occur between the N-terminal end of the interacting helix of HPr and helix H2 of the α domain and the loop connecting strand β3 and helix H6 of the α/β domain of EIN. In our model, contacts occur between the entire interacting helix, as well as the helical loop, of HPr and helices H2, H3, and H4 of the α domain, in accordance with the observed chemical shift changes induced upon complexation.

Our NMR data and the model of the interaction between EIN and HPr shown in Figure 5 suggest an important role for the kink between helices H2 and H2′ in the function of EI. Backbone amide residues for Leu 80, Asp 82, Glu 83, and Glu 84 are among the seven residues which experience the largest backbone chemical shift changes upon complex formation, suggesting that a hinge motion at that kink may occur. Interestingly, Asp 82 is conserved in all known EI sequences (with the exception of EI from *Bacillus subtilis* for which most of helix H2 is missing), with neighboring residues being either identical, near identical, or substituted by a proline, clearly indicating the functional necessity for a kink at that position. In addition, the two residues in helix H3 (Gly 110 and Gln 111) and the two in helix H4 (Gly 134 and Lys 135), which are spatially close to the kink region between helices H2 and H2′, are also among the residues exhibiting the largest chemical shift perturbations upon complexation. These two regions both contain glycine residues which are known for their potential to adopt a large range of backbone conformations and for their generally higher intrinsic flexibility. We therefore suggest that the two pairs of helices in the α domain of EIN can open slightly, akin to a paper clip, primarily at the hinge connecting helices H2 and H2′, in order to allow the helical loop and interacting helix of HPr to optimally interact with helices H2, H3, and H4 of the α domain, thereby permitting His 15 at the N-terminus of the HPr interaction helix to come sufficiently close to His 189 at the domain interface of EIN to allow phosphoryl transfer to take place. At this point it should be stressed that the proposed model is solely based on indirect observations and that a complete understanding of the mechanism of phosphoryl transfer from EIN to HPr and the

accompanying conformational changes will have to await a three-dimensional structure of the EIN/HPr complex. Work is currently underway in our laboratory to solve the structure of this complex by NMR.

ACKNOWLEDGMENT

We thank Frank Delaglio for software and Rolf Tschudin for technical support.

REFERENCES

Anderson, J. W., Bhanot, P., Georges, F., Klevit, R. E., & Waygood, E. B. (1991) *Biochemistry 30*, 9601−9607.

Carson, M. (1987) *J. Mol. Graphics 5*, 103−106.

Chauvin, F., Fomenkov, A., Johnson, C. R., & Roseman, S. (1996) *Proc. Natl. Acad. Sci. U.S.A. 93*, 7028−7031.

Chen, Y., Reizer, J., Saier, M. H., Jr., Fairbrother, W. J., & Wright, P. E. (1993) *Biochemistry 32*, 32−37.

Delaglio, F., Grzesiek, S., Vuister, G. W., Zhu, G., Pfeifer, J., & Bax, A. (1995) *J. Biomol. NMR 6*, 277−293.

Emerson, S. D., Madison, V. S., Palermo, R. E., Waugh, D. S., Scheffler, J. E., Tsao, K.-L., Kiefer, S. E., Liu, S. P., & Frey, D. C. (1995) *Biochemistry 34*, 6911−6918.

Fairbrother, W. J., Gippert, G. P., Reizer, J., Saier, M. H., & Wright, P. E. (1992) *FEBS Lett. 296*, 148−152.

Garrett, D. S., Powers, R., Gronenborn, A. M., & Clore, G. M. (1991) *J. Magn. Reson. 95*, 214−220.

Garrett, D. S., Seok, Y.-J., Liao, D.-I., Peterkofsky, A., Gronenborn, A. M., & Clore, G. M. (1997) *Biochemistry 36*, 2517−2530.

Gronenborn, A. M., & Clore, G. M. (1993) *J. Mol. Biol. 233*, 331−335.

Grzesiek, S., & Bax, A. (1993) *J. Am. Chem. Soc. 115*, 12593−12594.

Grzesiek, S., Bax, A., Clore, G. M., Gronenborn, A. M., Hu, J.-S., Kaufman, J., Palmer, I., Stahl, S. J., & Wingfield, P. T. (1996) *Nat. Struct. Biol. 3*, 340−345.

Hammen, P. K., Waygood, E. B., & Klevit, R. E. (1991) *Biochemistry 30*, 11842−11850.

Herzberg, O., & Klevit, R. E. (1994) *Curr. Opin. Struct. Biol. 4*, 814−822.

Herzberg, O., Reddy, P., Sutrina, S., Saier, M. H., Reizer, J., & Kapadia, G. (1992) *Proc. Natl. Acad. Sci. U.S.A. 89*, 2499−2503.

Jia, Z., Quail, J. W., Waygood, E. B., & Delbaere, L. T. J. (1993) *J. Biol. Chem. 268*, 22490−22501.

Jones, T. A. (1978) *J. Appl. Crystallogr. 11*, 268−272.

Klevit, R. E., & Waygood, E. B. (1986) *Biochemistry 25*, 7774−7781.

Liao, D.-I., Kapadia, G., Reddy, P., Saier, M. H., Reizer, J., & Herzberg, O. (1991) *Biochemistry 30*, 9583−9594.

Liao, D.-I., Silverton, E., Seok, Y.-J., Lee, B. R., Peterkofsky, A., & Davies, D. R. (1996) *Structure 4*, 861−872.

Nicholls, A. J., Sharp, K. A., & Jonig, B. (1991) *Proteins: Struct., Funct., Genet. 11*, 281−296.

Pelton, J. G., Torchia, D. A., Meadow, N. D., & Roseman, S. (1993) *Protein Sci. 2*, 543−558.

Postma, P. W., Lengeler, J. W., & Jacobson, G. R. (1993) *Microbiol. Rev. 57*, 543−594.

Rajagopal, P., & Klevit, R. E. (1994) *Tech. Protein Chem. 5*, 439−445.

Reddy, P., Fredd-Kuldell, N., Liberman, E., & Peterkofsky, A. (1991) *Protein Expression Purif. 2*, 179−187.

Seok, Y.-J., Lee, B. R., Zhu, P.-P., & Peterkofsky, A. (1996) *Proc. Natl. Acad. Sci. U.S.A. 93*, 347−351.

Shuker, S. B., Hajduk, P. J., Meadows, R. P., & Fesik, S. W. (1996) *Science 274*, 1531−1534.

van Nuland, N. A. J., Kroon, G. J. A., Dijkstra, K., Wolters, G. K., Scheek, R. M., & Robillard, G. T. (1993) *FEBS Lett. 315*, 11−15.

van Nuland, N. A. J., Hangyi, I. W., van Schaik, R. C., Berendsen, H. J. C., Van Gunsteren, W. F., Scheek, R. M., & Robillard, G. T. (1994) *J. Mol. Biol. 237*, 544−559.

van Nuland, N. A. J., Boelens, R., Scheek, R. M., & Robillard, G. T. (1995) *J. Mol. Biol. 246*, 180−193.

Weigel, N., Kukuruzinska, M. A., Nakazawa, A., Waygood, E. B., & Roseman, S. (1982a) *J. Biol. Chem. 257*, 14477−14491.

Weigel, N., Powers, D. A., & Roseman, S. (1982b) *J. Biol. Chem. 257*, 14499−14509.

Wittekind, M., Rajagopal, P., Branchini, B. R., Reizer, J., Saier, M. H., & Klevit, R. E. (1992) *Protein Sci. 1*, 1363−1376.

Worthylake, D., Meadow, N. D., Roseman, S., Liao, D.-I., Herzberg, O., & Remington, S. J. (1991) *Proc. Natl. Acad. Sci. U.S.A. 88*, 10382−10386.

BI970221Q